

Iron, nutrient, and phytoplankton distributions in Oregon coastal waters

Zanna Chase,^{1,2,3} Alexander van Geen,¹ P. Michael Kosro,⁴ John Marra,¹ and Patricia A. Wheeler⁴

Received 18 May 2001; revised 5 December 2001; accepted 14 March 2002; published 25 October 2002.

[1] The relationship between iron and nitrate concentrations was examined off the coast of Oregon during the upwelling season. Surface Fe and N (nitrate + nitrite) concentrations measured underway by flow injection analysis ranged from <0.3 to 20 nmol L^{-1} and <0.1 to $30 \text{ } \mu\text{mol L}^{-1}$, respectively. Total dissolvable Fe concentrations, measured in unfiltered, acidified samples in surface waters and in vertical profiles, ranged from <0.3 to 300 nmol L^{-1} . Surface water Fe and N concentrations were highly variable and uncoupled. Our observations indicate two dominant sources of Fe to Oregon coastal waters: Slope or shelf sediments and the Columbia River. Sedimentary iron, probably largely in the particulate form, appears to be added to surface waters through wind-induced vertical mixing during strong winds, through thickening of the bottom mixed layer during relaxation or downwelling favorable wind conditions, and through outcropping of shelf bottom waters during upwelling events. The existence of multiple iron sources and the generally high iron concentrations may explain why the distribution of phytoplankton, measured both remotely (by Sea-viewing Wide Field-of-view Sensor) and underway (by *in vivo* fluorescence), appeared to be driven primarily by physical dynamics and was not strongly linked to the distribution of iron. Nevertheless, at some offshore stations where underway Fe concentrations were $<0.3 \text{ nmol L}^{-1}$, underway measurements of the physiological state of phytoplankton by fast repetition rate fluorometry were consistent with mild iron stress, and cross-shelf nutrient distributions were consistent with iron regulation of the magnitude of phytoplankton blooms. **INDEX TERMS:** 4875 Oceanography: Biological and Chemical: Trace elements; 4805 Oceanography: Biological and Chemical: Biogeochemical cycles (1615); 4853 Oceanography: Biological and Chemical: Photosynthesis; 4845 Oceanography: Biological and Chemical: Nutrients and nutrient cycling; **KEYWORDS:** iron, Oregon, upwelling, nutrients, coastal, chlorophyll

Citation: Chase, Z., A. van Geen, P. M. Kosro, J. Marra, and P. A. Wheeler, Iron, nutrient, and phytoplankton distributions in Oregon coastal waters, *J. Geophys. Res.*, 107(C10), 3174, doi:10.1029/2001JC000987, 2002.

1. Introduction

[2] Because of their proximity to shelf sediments and terrestrial sources, coastal waters are typically enriched in iron relative to the open ocean [Johnson *et al.*, 1997]. Yet recent work in the California coastal upwelling system [Hutchins and Bruland, 1998; Hutchins *et al.*, 1998] has demonstrated that the addition of iron to incubation bottles from some coastal regions stimulates phytoplankton growth and nitrate consumption much as it does in open ocean high-nutrient, low-chlorophyll (HNLC) regions [e.g., Coale *et al.*, 1996]. Thus, iron is potentially an important variable

controlling phytoplankton biomass and community composition [Bruland *et al.*, 2001; Johnson *et al.*, 2001] in productive coastal upwelling systems.

[3] Most of the work to date on iron in coastal upwelling systems has focused on waters off central California. Dissolved iron concentrations in upwelling source waters (depth of $\sim 150 \text{ m}$, $\sim 175 \text{ km}$ offshore) of the California Current are relatively low ($<1 \text{ nmol L}^{-1}$) [Martin and Gordon, 1988], which suggests that, in contrast to its effect on the macronutrients, upwelling of deep water does not significantly enrich surface waters in iron. Additional potential iron sources to the coastal ocean include shelf sediments, wind-blown dust, and riverine inputs. Given the relatively high precipitation north of central California, and the prevailing alongshore wind direction, aeolian inputs of iron are expected to be small. The concentration of dissolved iron in river water can be several orders of magnitude greater than open ocean concentrations [Boyle *et al.*, 1977]. However up to 95% of riverine filterable iron can be lost through estuarine processes such as flocculation and precipitation [Boyle *et al.*, 1977; Mayer, 1982a], so even large rivers may contribute very little dissolved iron to the

¹Lamont-Doherty Earth Observatory of Columbia University, Palisades, New York, USA.

²Also at Department of Earth and Environmental Sciences, Columbia University, Palisades, New York, USA.

³Now at the Monterey Bay Aquarium Research Institute, Moss Landing, California, USA.

⁴College of Oceanic and Atmospheric Sciences, Oregon State University, Corvallis, Oregon, USA.

coastal ocean. Indeed, resuspended shelf sediments were found to be the dominant source of Fe to surface waters off central California, even during periods of increased river runoff [Johnson *et al.*, 1999].

[4] The west coast of North America has considerable alongshore variability in upwelling characteristics, climate and shelf geometry, all of which could affect Fe inputs. For instance, the continental shelf off Oregon, defined by the 200 m isobath, varies from a minimum width of 11 km, just off Cape Blanco (42°N) to a maximum of 78 km, at Heceta Bank (44.2°N), and is generally wider than the shelf off California. Furthermore, in the summer, surface waters off Oregon are strongly influenced by freshwater input from the Columbia River, which has its maximum discharge in June, when the plume is directed almost exclusively southward over the Oregon shelf.

[5] This paper describes high-resolution surface, and bottle-based vertical distributions of key chemical and biological properties measured off southern Oregon and northern California in July 1999. The objective of this study was to understand the physical processes governing iron inputs during the upwelling season, in order to better understand the development of HNLC conditions in the coastal ocean. The specific hypotheses pertaining to this region include: 1) Low levels of iron can limit the size of phytoplankton blooms and nutrient consumption; 2) Shelf sediments are an important source of Fe to surface waters; 3) The Columbia River is an important source of Fe to surface waters and 4) Iron and macronutrients are input to surface waters by different mechanisms and at different times.

2. Methods

2.1. Sample Collection

[6] Sampling took place off the Oregon and California coasts between July 3 and July 9, 1999, aboard the R/V *Wecoma*. Time, position, bottom depth, wind speed, downwelling solar radiation (285–2800 nm), flow through sea surface temperature (SST) and flow through salinity were recorded as 1 min averages by the ship's data logger (XMIDAS). Shipboard ADCP data were collected and processed as described by Kosro [2002]. When the ship was underway at 10 knots, a continuous stream of near-surface (~1–3 m depth), trace metal clean seawater was obtained for iron and nitrate analyses using a brass 'fish' (a bathythermograph) towed over the side of the ship [Boyle *et al.*, 1982; van Geen *et al.*, 2000; Vink *et al.*, 2000]. The fish was suspended from a boom about 5 m off the port side, and its torpedo shape helped maintain the tubing intake pointing forward and into the water. Through its ~1 min transit from the ocean to a class 100 laminar flow bench, the pumped seawater was only in contact with Teflon[®]-lined tubing, with the exception of a ~50 cm length of silicone tubing (9.5 mm ID; Masterflex[®]) in a large peristaltic pump. All tubing was leached with 1.2 N HCl for at least 24 h and then rinsed thoroughly with ultrapure MQ water (18.2 MΩ, Millipore) prior to use. The pumped flow was normally directed into a 50 mL overflowing graduated cylinder within the flow bench, from which a flow for underway iron and nitrate measurements was drawn by a peristaltic pump. By switching acid-cleaned Teflon[®] valves this flow was occasionally diverted to fill archive bottles for future

analysis. The pumping system was turned off during CTD intensive transects. These lines were in most cases immediately resampled after the CTD casts as a continuous transect for underway measurements.

[7] Profile samples for Fe analysis were collected in acid-leached high-density polypropylene bottles from Niskin bottles (General Oceanics) modified for trace metal sampling by acid leaching, replacing inner springs with C flex tubing, and viton o rings with fluorosilicone O rings. A standard metal rosette frame and hydrowire were used. All discrete samples, including those from the underway pumping system, were acidified at sea by the addition of 1 mL L⁻¹ of concentrated Seastar HCl and analyzed within 7 months by the flow injection method described below.

2.2. Flow Injection Analysis

[8] Nitrate and iron were detected colorimetrically by flow injection analysis using a three-channel fiber-optic spectrophotometer (Ocean Optics). The sensitivity of both methods was increased with long path length spectrophotometric cells (LPC) using the Teflon AF-2400 (Biogeneral) liquid core waveguide approach described by Waterbury *et al.* [1997]. A 10-port injection valve (VICI) was used to control sample and reagent flow, which permitted both the Fe and NO₃ sample loops to be filled simultaneously. A 10-port selection valve (Cheminert) was used to direct either standards or the sample stream into the system, with at least 4 standards run typically every hour. Surface seawater samples were injected every 80 seconds. Standards, run in triplicate, were mixed solutions of iron and cleaned (Chelex-100) nitrate, acidified with 1 mL L⁻¹ HCl as described above for discrete samples. Nitrate was undetectable in the iron stock solution and iron was undetectable in the cleaned nitrate stock solution.

2.2.1. Iron

[9] Iron was measured using a modification of the method of Measures *et al.* [1995], with a 10 cm LPC. We did not preconcentrate the samples, in order to reduce sampling time, and thereby maximize the spatial resolution of sampling, and to avoid cross contamination in this region of strong gradients in surface Fe concentrations. To further simplify the system and minimize contamination, the sample stream was neither filtered nor acidified before injection. The lack of filtration caused clogging of the valves on several occasions in nearshore waters, which lead to system downtime. Unacidified MQ water (UA-MQ) was run with each set of standards. Usually, the absorbance of the UA-MQ was less than that of acidified MQ water, presumably because acidified MQ was leaching some adsorbed Fe from the system. Since the seawater stream was unacidified, we subtracted the UA-MQ peak from every sample peak as a blank value and took the sensitivity (absorbance per mole Fe) from the slope of the standard curve using acidified standards. Most of the time the UA-MQ blank was not detectable above the baseline. The detection limit was ~0.3 nmol L⁻¹, based on variability of the blank. The precision, based on triplicate analyses of standards, was 1–6%. The response of the detector for Fe was linear up to a concentration of 100 nmol L⁻¹. Drift over an hour separating standards, both in terms of blank and sensitivity, was generally <20%, and was assumed to be linear as a function of time.

[10] The same flow injection system was used for analyzing discrete samples for iron. Five of the ports on the 10-

port selection valve were dedicated to samples, and flushed thoroughly between runs. Samples containing Fe above the linear range of the method were diluted with acidified MQ and rerun.

[11] The current chemical Fe literature is confusing because of the use of different terminology resulting from the wide variety of methods used to analyze Fe, and the similarly wide variety of preanalysis sample treatments employed. In this paper we discuss both discrete samples, which were acidified with 2 mL L^{-1} 12N HCl and stored at least 2 months prior to analysis, and underway samples, unacidified and analyzed inline at a reaction pH of 6.4. At the low pH (~ 2) of the unfiltered samples, organically bound Fe, colloidal Fe, and some, if not all, particulate Fe would certainly be released into solution during storage. We will therefore refer to the discrete analyses as 'dissolvable Fe' (dFe). This probably represents the maximum potentially bioavailable iron in the system over biologically relevant timescales. Our terminology is similar to that employed by *Bruland and Rue*, [2001] when referring to the analysis of unfiltered, acidified, stored, samples. This should not be confused with the "DI Fe" used by *Martin and Gordon* [1988] to denote dissolved ($0.4 \mu\text{m}$) Fe. Note that the term "dissolvable Fe" has also been used to describe shipboard Fe measurements by FIA of unfiltered samples following a brief period of acidification to pH ~ 3 [*Obata et al.*, 1997; *Johnson et al.*, 1999]. This "dFe" is closer to the "underway Fe" described in this paper, although we omitted the brief acidification step.

[12] If we can be reasonably confident that acidified, stored samples return something close to the 'total' (dissolved + particulate) Fe in a water sample, the fraction and nature of Fe detected by other methods, including the underway method used here, is far less certain and is often simply operationally defined. The Fe that we measured underway in an unacidified, unfiltered stream, at a reaction pH of 6.4 for ~ 40 seconds most likely includes only the most reactive Fe, and therefore represents a minimum estimate of bioavailable Fe. Preliminary experiments using a large excess of EDTA as a chelator suggest organically bound Fe is not detected under these conditions. However, tests against EDTA-complexed Fe may be misleading, since these complexes are not typical of naturally occurring iron binding ligands, which tend to have lower concentrations and lower conditional stability constants than EDTA [*Morel and Hering*, 1993]. Despite this acknowledged uncertainty in the nature of the iron detected by the underway measurements, we believe they are still informative, particularly in showing regional differences within this study area. Unfortunately, differences in methodology make it difficult to compare our results with those of other workers using different methods. Even the work of *Vink et al.* [2000], whose methodology most closely resembles ours, is not directly comparable, because inline acidification was used in the Vink et al. study (as by *Johnson et al.* [1999]), and in addition their samples were preconcentrated before injection.

2.2.2. Macronutrients

[13] Nitrate + nitrite (N) was measured underway, as described above using the standard azo dye colorimetric method [e.g., *Anderson*, 1979]. The detection limit was $0.1 \mu\text{mol L}^{-1}$ and the precision 1–6%. The response was linear

to $100 \mu\text{mol L}^{-1}$. Nitrate (N), phosphate (P), and silicic acid (Si) in surface waters were also measured in the laboratory in discrete samples collected from the underway pumping system using a commercial flow injection system (Lachat QuikChem 8000) with standard colorimetric methods, as by *van Geen et al.* [2000]. Profile samples for macronutrient analyses were collected from the CTD rosette and were neither filtered, nor acidified, and were stored frozen. Macronutrients from the CTD profiles samples were analyzed by standard wet chemical methods according to protocols of *Gordon et al.* [1995] using an Alpkem RFA-300.

2.3. Fluorometry

[14] In vivo fluorescence was measured underway from the ship's flow through intake (~ 3 m depth) with a Turner Designs (model 10-AU) fluorometer. The in vivo fluorescence signal was calibrated with extracted chlorophyll sampled from the instrument's outlet and extracted chlorophyll from surface and 10 m Rosette samples at CTD stations, interpolated to 3 m.

[15] The fast repetition rate fluorometer (Chelsea Instruments) was run in underway mode, from the same sample stream as the underway fluorometer. We used a flash sequence of 100 saturation flashes of $1.1 \mu\text{s}$ duration, separated by $\sim 2.8 \mu\text{s}$ followed by 20 relaxation flashes of $1.1 \mu\text{s}$ duration, separated by $51.6 \mu\text{s}$. Each sample was an average of 10 sequences. A constant gain of 1 was used throughout the cruise. Optical surfaces were cleaned daily. Data were reduced using the Chelsea Instruments software to obtain the initial, or minimal (F_0) and maximal (F_m) fluorescence yield. From these parameters we derive the ratio $F_v/F_m = (F_0 - F_m)/F_m$, which is the maximum change in the quantum yield of fluorescence, a quantitative measure of the efficiency of photosystem II.

3. Results

3.1. Physical Setting

[16] An image from the Advanced Very High Resolution Radiometer (AVHRR) on July 3 shows cool water nearshore throughout the cloud-free study area, with the coldest waters south of Cape Blanco (43°N ; Figure 1). An 8 day composite image from the Sea-viewing Wide Field-of-view Sensor (SeaWiFS; data obtained through the Goddard DAAC at http://daac.gsfc.nasa.gov/data/data_set/SEAWIFS/) (Figure 1b) shows a visual association between cool SST in the AVHRR image and high phytoplankton biomass, despite the difference in temporal coverage between the two images (Figure 1). South of 42°N both SST and chlorophyll occurred in distinct plumes. Many of the features of the SST and chlorophyll distributions, including a seaward extension of cool, chlorophyll-rich water south of Cape Blanco (Figure 1), can be related to the acoustic Doppler velocity at 17 m. The surface velocity field defined the trajectory of a coastal jet, which can be followed from 45°N , where it was present nearshore, to $\sim 44.2^\circ\text{N}$, where it began to separate from the coast, then returned shoreward at 43°N , and finally moved offshore south of Cape Blanco (41°N), similar to the flow described by *Barth et al.* [2000] for a previous year. The flow south of 42°N is particularly energetic and complex, and is consistent with the intrusion of

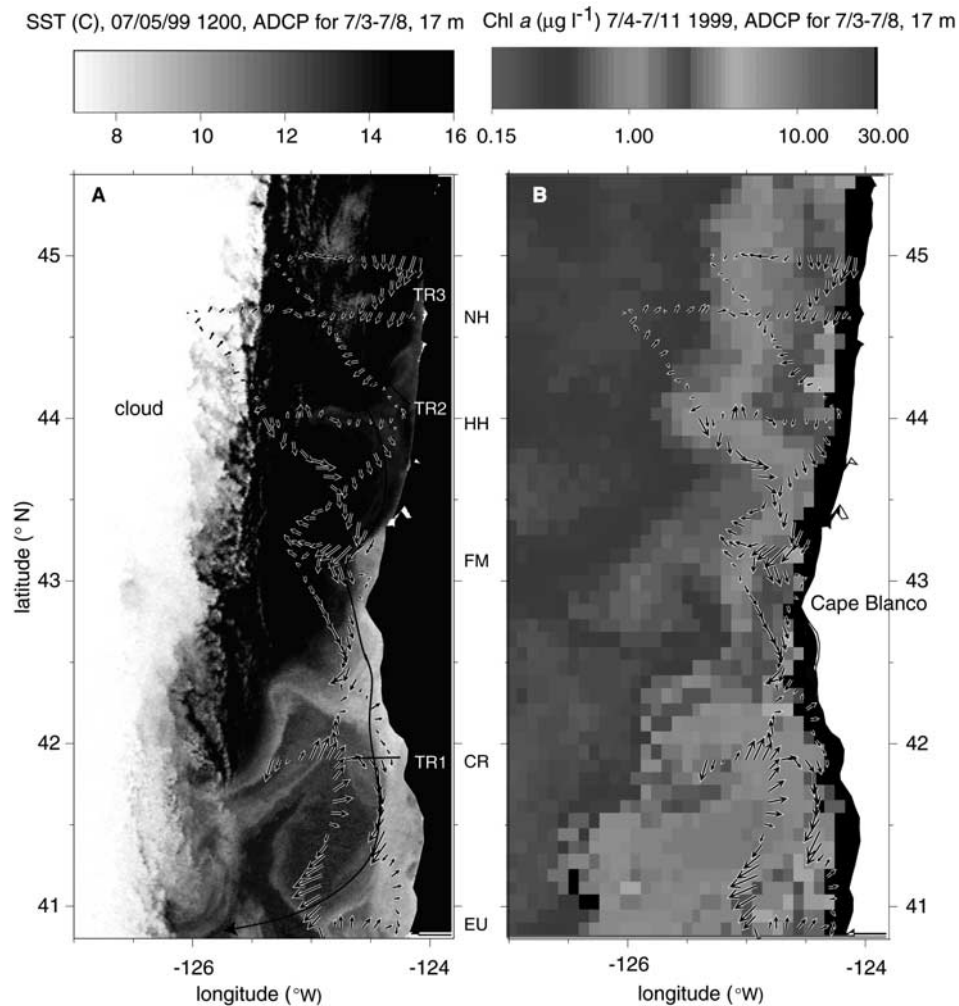


Figure 1. ADCP velocity vectors (longest arrow represents 42 cm/s) at 17 m between 3 and 8 July 1999 overlaid on satellite-derived (a) sea surface temperature ($^{\circ}\text{C}$) from 5 July and (b) an 8 day (7/4–7/11) composite of satellite-derived chlorophyll *a* concentration ($\mu\text{g L}^{-1}$). Chlorophyll is displayed on a logarithmic scale. There are no chlorophyll data in the black regions near the coast. A probable path of the coastal current has been subjectively drawn through the velocity vectors in Figure 1a. The locations of three transects where high-resolution data are examined more closely are also indicated in Figure 1a. Initials along the coast indicate the standard sampling lines of the Oregon GLOBEC program. See color version of this figure at back of this issue.

relatively warm, low-chlorophyll waters near the shelf break, evident in the AVHRR and SeaWiFS images (Figure 1).

[17] Wind vectors from three stations within the study area were broadly coherent (by inspection), and demonstrate the dominance of upwelling favorable winds (equatorward, negative) during this season (Figure 2). However, wind relaxation events did occur, for example at the beginning of the cruise (07/03–07/04), on 07/07 north of 43°N , and on 07/09 at 41°N (Figures 2a and 2b).

3.2. Regional Pattern of Near-Surface Properties

[18] Cape Blanco defined a boundary between two distinct regimes in SST, surface salinity and surface chlorophyll *a* (Figure 1 and Figures 3a, 3b, and 3c). Waters to the north of Cape Blanco, seaward of the 50 m isobath, were warm (up to 17°C), fresh (salinity as low as 23 psu) and contained relatively little chlorophyll ($<2 \mu\text{g L}^{-1}$). Upwelling centers

of cool SST, high salinity and elevated chlorophyll were observed near the HH line (44°N) and north of the NH line (44.7°N), but these were restricted to within the 200 m isobath (Figure 3). South of Cape Blanco, very cold (9°C), salty (up to 34 psu) and chlorophyll-rich ($\sim 20 \mu\text{g L}^{-1}$) waters were observed along the coast. Cool ($<13^{\circ}\text{C}$), salty (up to 33.5 psu), chlorophyll-rich ($5\text{--}10 \mu\text{g L}^{-1}$) waters extended seaward of the 1000 m isobath in this region. The very cold SSTs and high salinity measured near the CR line on 07/05 are a clear indication of strong upwelling. Winds recorded to the north and south of the CR line (42°N) at this time were indeed upwelling favorable (Figures 2b and 2c), but they were not particularly strong. This apparent discrepancy between wind and upwelling strength, as inferred from tracer distributions, can be attributed to the enhanced shoaling of the pycnocline, for a given wind stress, as a current flows cyclonically around a prominent feature, such as Cape Blanco [Arthur, 1965].

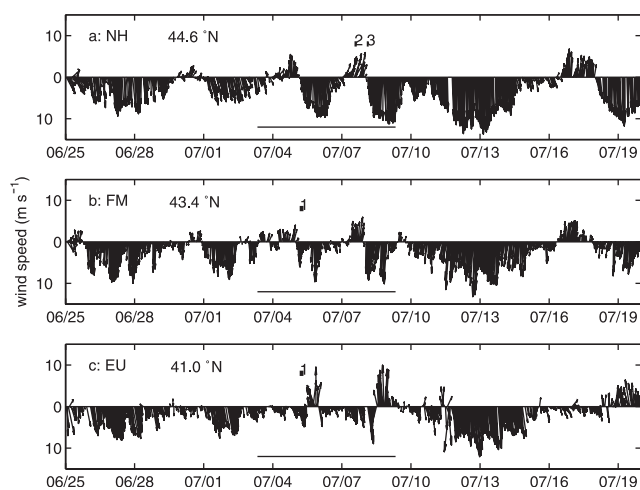


Figure 2. Wind vectors (m s^{-1}) measured from (a) near the NH line at the Newport buoy (44.6°N , 124.5°W ; NOAA buoy 46050), (b) near the FM line at the Cape Arago lighthouse (43.4°N , 124.4°W ; Station CARO3), and (c) near the EU line at the St George buoy (41.0°N , 124.4°W ; NOAA buoy 46027). The duration of the R/V *Wecoma* cruise is indicated by a thin line in all panels, and the approximate time of sampling along GLOBEC lines in the vicinity of each wind station is indicated by initials along this line. The time of the detailed transects in the vicinity of each wind station (TR1, TR2, and TR3; see Figure 1) is indicated by a bold line and numeral in each panel. Note that TR1, along the CR line, is located between the FM and the EU lines and TR2 is between the NH and FM lines. Wind data are available from the National Data Buoy Center (<http://www.ndbc.noaa.gov/Maps/Northwest.shtml>).

[19] High concentrations of N tended to be associated with nearshore, cold, high-salinity waters (Figures 3 and 4), consistent with a primary supply from upwelling. In general there was good agreement between underway and discrete measurements of N ($r^2 = 0.83$; $n = 65$; Figures 4a, 4b, and 5a). The generally higher values in discrete samples could be due to acid solubilization of particulate organic nitrogen included in the unfiltered discrete samples; some of the largest outliers were indeed from regions of high chlorophyll (Figure 5a). Some of the scatter in this relationship may also be due to smearing of signals in the underway system and the difficulty of precisely time matching underway and discrete samples, especially in regions of strong horizontal gradients in N.

[20] The distribution of Si, in contrast to N, was not well delimited by Cape Blanco. Si-rich waters were present both south of Cape Blanco, in the cold, salty water along the coast near the CR line, and also north of Cape Blanco, in warm, fresh waters as far as the 1000 m isobath (Figure 3d). The presence of the Columbia River plume was indicated by the very low salinity (23–24 psu), high Si (up to $41 \mu\text{mol L}^{-1}$) and warmer SSTs [Park *et al.*, 1972] measured offshore at the northern end of the cruise track. A riverine source of Si, in addition to the upwelling source, probably explains why the distribution of Si was poorly delimited by Cape Blanco.

[21] Of the underway observations in this study, 55%, were of $\text{Fe} < 1 \text{ nmol L}^{-1}$, and of samples containing more than $10 \mu\text{mol L}^{-1}$ N ($n = 105$), 20% had $\text{Fe} < 0.5 \text{ nmol L}^{-1}$.

Iron concentrations measured in stored, acidified samples collected from the underway pumping system were up to 20-fold higher than underway measurements by FIA (Figures 4c, 4d, and 5b). The difference between the two measurements was greatest in shallow, nearshore waters (Figures 4c and 4d), which are more likely to contain elevated levels of particulate Fe [Johnson *et al.*, 1997], and possibly colloidal Fe, which would have been partly or completely solubilized by acidification. Underway Fe concentrations were not well correlated with either salinity (Figure 6b), N (Figure 6c) or SST (not shown).

[22] The distribution of Fe resembled the distribution of Si more so than the distribution of N: High Fe was observed in cold, salty waters along the coast south of Cape Blanco, and also in low salinity waters of the Columbia River plume, particularly along 45°N (Figures 4c and 4d). Considering all of the data together, discrete Fe concentrations were better correlated with Si than with N or P (Figure 7). Phosphate concentrations closely followed nitrate (Figure 7f), with a slight excess of P over N, as observed in other coastal upwelling systems [Brzezinski *et al.*, 1997]. The poorer correlation between Si and N and P, compared to the strong correlation between N and P (Figures 7b, 7d, and 7f) again most likely reflects the fact that Si has both an upwelling and a riverine source.

3.3. Vertical Distributions

[23] Selected profiles of density, N, chlorophyll *a* and dFe are shown in Figure 8. In each case, an offshore station, the upwelling source region, is paired with a nearshore station along the same sampling line. All measurements of Fe in vertical profiles were from discrete samples (i.e., total dissolvable iron, dFe). In general, less than 20 hours separated sampling the offshore and the nearshore stations, except along the NH line, where the offshore station was sampled 4 days before the nearshore station.

[24] The distinction between waters to the north and south of Cape Blanco is visible in the offshore density profiles, with waters north of Cape Blanco being far more stratified than those to the south (CR and EU lines) (Figure 8). The distribution of nitrate was generally related to density, presumably through wind-driven shoaling of the isopycnal surfaces. The densest water ($\sigma_{\theta} = 26$) and highest nitrate ($>20 \mu\text{mol L}^{-1}$) was found in the deepest water at all stations, and the stations with highest surface density (NH and CR, nearshore) had the greatest surface nitrate (Figure 8). Low surface nitrate at the nearshore EU station, despite high density, suggests some consumption of N had occurred.

[25] In contrast, the distribution of iron was not obviously related to density (Figure 8). As expected, offshore dFe concentrations were generally lower than nearshore concentrations at all depths. Although concentrations near the detection limit were measured just below the surface on the NH and FM lines, dFe concentrations greater than 10 nmol L^{-1} were observed at depth at the offshore stations on all but the NH line, with $\text{dFe} > 30 \text{ nmol L}^{-1}$ on the HH, CR, and HH lines (Figure 8). These “offshore” dFe concentrations are an order of magnitude greater than those measured a similar distance from shore off Monterey Bay [Martin and Gordon, 1988; Johnson *et al.*, 1999]. It is difficult to imagine that methodological differences, for

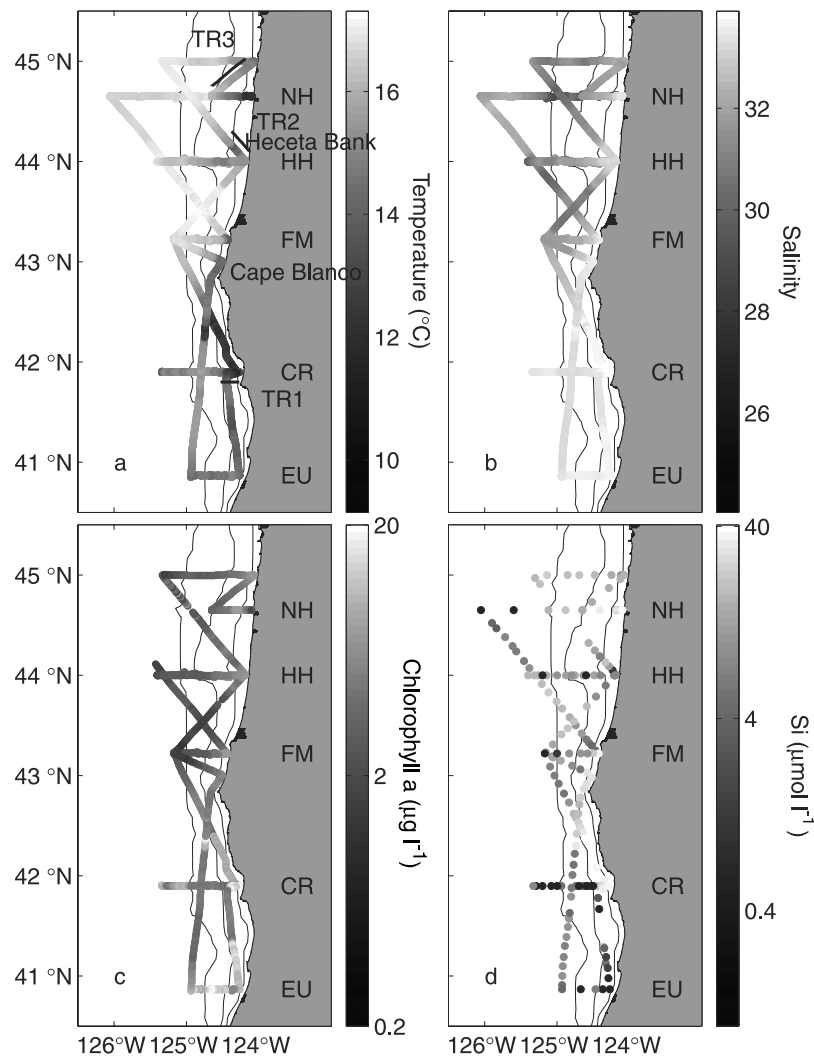


Figure 3. Surface water properties measured off Oregon during July 3–8, 1999. (a) Temperature ($^{\circ}\text{C}$), (b) salinity, and (c) chlorophyll *a* ($\mu\text{g L}^{-1}$, estimated from in vivo fluorescence) were measured continuously while the ship was underway. (d) Silicate (silicic acid) was measured in discrete, acid-preserved samples in the laboratory. Where transects were covered twice during the cruise, the later data are plotted over the earlier data. Note the logarithmic color scale used for chlorophyll *a* and silicate concentrations. Contour lines represent the 50, 200, and 1000 m isobaths. See color version of this figure at back of this issue.

example, in the strength and duration of acidification, could account for such a large difference between the two regions.

[26] Phytoplankton biomass, which was included in the unfiltered water samples used for Fe analysis, accounted for a small fraction of the total Fe measured in most profile samples. For example, assuming at the high end, as much as $50 \mu\text{gC}:\mu\text{gchl}a$ [Parsons *et al.*, 1977] and as much as $100 \mu\text{molFe}:\text{molC}$ [Sunda and Huntsman, 1995] for coastal phytoplankton, $6 \mu\text{g L}^{-1}$ of chlorophyll *a* yields at most only 5 nmol L^{-1} Fe. Thus, while phytoplankton biomass could account for most of the Fe in surface waters from the offshore stations (Figure 8), it can account for at most 3% of the high dFe concentrations found nearshore, or at depth at some of the offshore stations (e.g., HH, CR, and EU).

[27] At two nearshore stations along the NH line, dFe and beam attenuation (particle concentration) had similar profile shapes, both with a middepth minimum (Figure 9), suggest-

ing an association between the Fe and the particulate matter. The most obvious explanation is that the Fe is associated with lithogenic particulate matter resuspended from sediments [Martin and Gordon, 1988; Johnson *et al.*, 1999]. Although chlorophyll (fluorescence) does not contribute significantly to dFe loads (see discussion above), it does contribute to beam attenuation [Small and Curl, 1968]. The presence of chlorophyll at the surface therefore complicates the relationships between beam attenuation, particulate matter, and Fe. We have used the relationship between beam attenuation and fluorescence, derived from all CTD casts (not shown), to correct beam attenuation for the attenuation associated with fluorescence. When corrected for chlorophyll, the beam attenuation signal is reduced at the surface, but not significantly at depth (Figure 9), and the middepth minimum in beam attenuation is preserved. This suggests that the pronounced middepth minimum in dFe is indeed linked to the

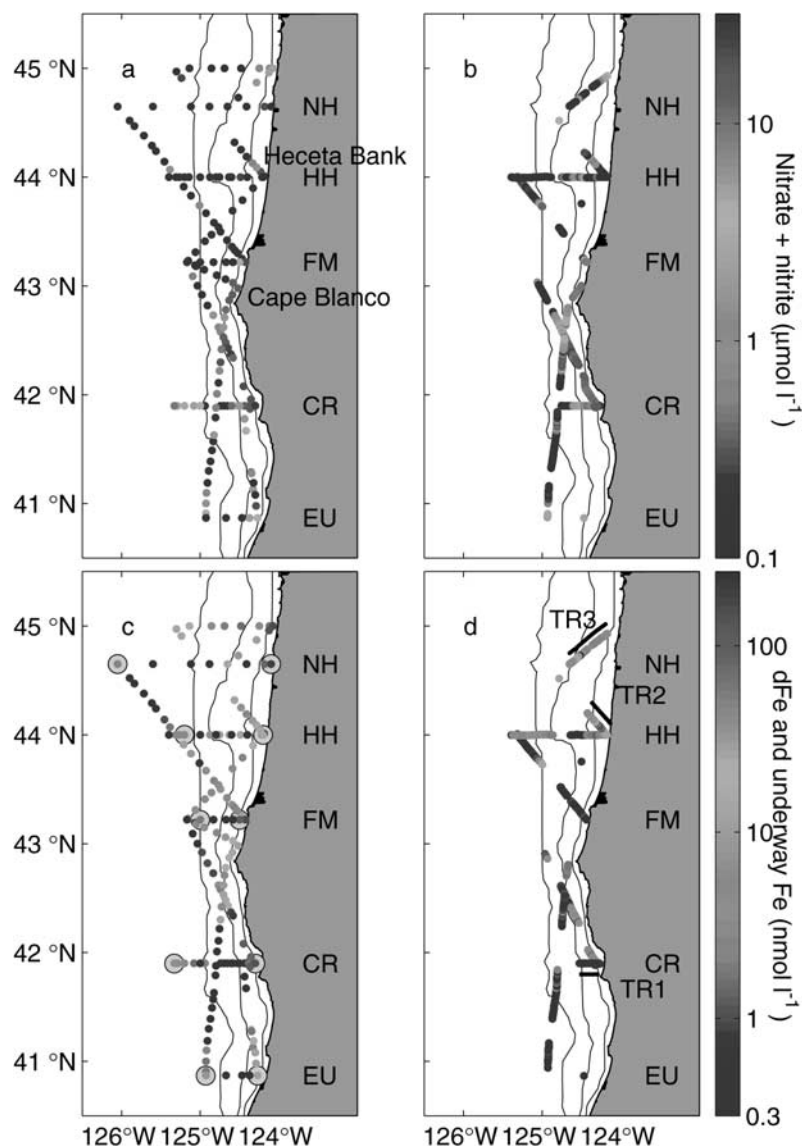


Figure 4. Surface water concentrations of (a) and (b) nitrate + nitrite (N) ($\mu\text{mol L}^{-1}$) and (c) and (d) iron (nmol L^{-1}) off Oregon, July 3–8, 1999, measured in discrete, acidified (pH 2) samples collected from the underway pumping system or (unacidified) surface rosette samples (Figures 4a and 4c) and at sea by flow injection analysis, without filtration or acidification (Figures 4b and 4d). Note the logarithmic color scale. Gray circles in Figure 4c indicate the location of CTD stations where vertical profiles of N and Fe were obtained. See color version of this figure at back of this issue.

depth distribution of lithogenic particles. Note that although the two stations had approximately the same “nonchlorophyll” particle content near the surface, near-surface dFe was a factor of 2 lower at 9 km from shore compared to 5 km from shore (Figure 9). This may reflect either a seaward decrease in the concentration of nonparticulate Fe, or a seaward decrease in the Fe content of particulate matter.

3.4. High-Resolution Cross-Shelf Transects

[28] High-resolution, underway mapping is ideally suited to the coastal upwelling environment, where small-scale spatial variability is common [Chavez *et al.*, 1991]. Here we present three cross-shelf transects of underway data that cover the sampled area and a range of upwelling conditions (TR1,

TR2, and TR3; see Figures 1 and 3 for location). Discrete bottle data from these transects are reported in Table 1.

[29] Winds were upwelling favorable at the time of sampling TR1 (Figure 2), and the low SST, high N (up to $15 \mu\text{mol L}^{-1}$) and high salinity nearshore indicate active upwelling (Figure 10). However, iron concentrations measured underway were low ($<0.5 \text{ nmol L}^{-1}$). Maximum chlorophyll was found 15 km offshore, coincident with a region of lower N, but with no corresponding change in SST or salinity (Figure 10). From the difference between the observed N concentration ($6 \mu\text{mol L}^{-1}$), and that predicted based on the more conservative tracers, SST and salinity ($12 \mu\text{mol L}^{-1}$), we estimate a removal of about $6 \mu\text{mol L}^{-1}$ N by phytoplankton growth.

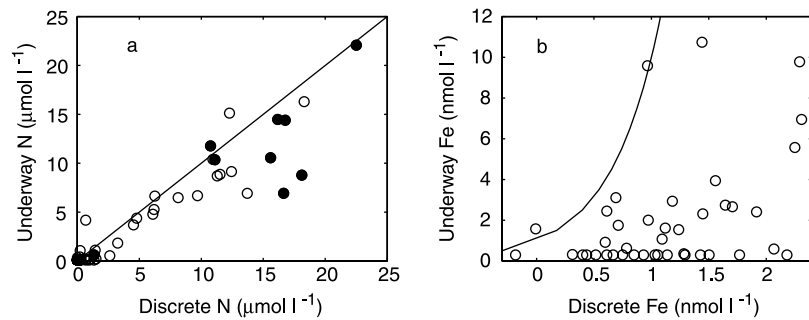


Figure 5. A comparison for (a) N and (b) Fe between measurements made underway by flow injection analysis on an unacidified sample stream and measurements from discrete bottle samples collected from the underway stream and stored acidified at pH 2 for 7 months prior to analysis. The 1:1 line is drawn for reference. Note the semilog scale in Figure 5b. Samples with chlorophyll *a* > 10 $\mu\text{g L}^{-1}$ are in solid circles.

[30] Transects TR2 and TR3 were sampled during upwelling favorable winds following about 2 days of downwelling (Figure 2a). Nearshore SSTs along TR2 were relatively warm (14°C) compared to SSTs further south (Figure 10), and surface water nitrate was undetectable within about 20 km from shore (Figure 10). Thus, the surface waters at TR2 had not yet been modified after ~ 12 hours of upwelling favorable local winds (Figures 6a and 6b), which is consistent with previous work showing it takes about 1 day for the upwelling circulation off Oregon to respond to the wind [Barber and Smith, 1981; Brink *et al.*, 1994]. However, in contrast to TR1, Fe concentrations along TR2 were high within 15 km from shore. Along TR2 there was a distinct cool ($11\text{--}13^{\circ}\text{C}$) patch, enriched in both N and Fe ($5\text{--}8 \mu\text{mol L}^{-1}$ N and $\sim 15 \text{ nmol L}^{-1}$ Fe) located between 20 and 30 km from shore (Figure 10). Inspection of

the ADCP velocity field at 17 m and an AVHRR image from July 3 (Figure 1a) suggests this cold feature may have been advected southwestward from the region of cool SST and high N nearshore on the NH line (Figure 3c).

[31] Waters along TR3 were influenced by the Columbia River plume, as seen by their low salinity (<31 psu; Figure 10), and high Si (Table 1). Along TR3, in contrast to TR2, decreasing SSTs and increasing salinity, N and Fe toward the coast indicate surface waters had begun to be modified by upwelling. The contrast between the cross-shelf distribution of SST, salinity and N along TR1 and TR3 suggests upwelling was more intense (faster and from greater depth) at TR1 than at TR3, although winds were more strongly equatorward at TR3 than at TR1 at the time of sampling (Figure 6). Underway Fe was about 10 times greater all along TR3 compared to TR1, while dFe was

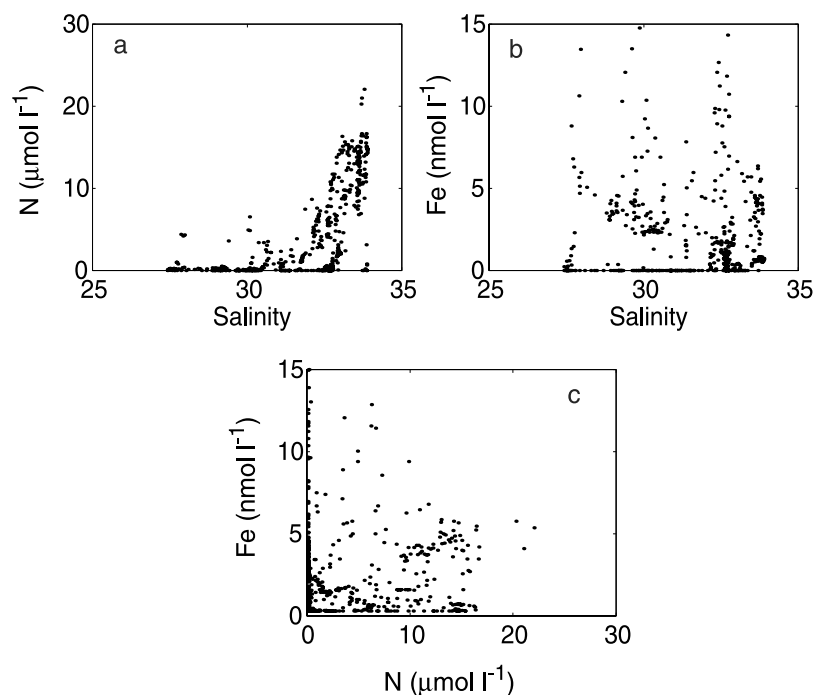


Figure 6. Scatterplot of surface salinity versus underway (a) nitrate + nitrite (N) and (b) Fe; (c) scatterplot of underway N versus underway Fe.

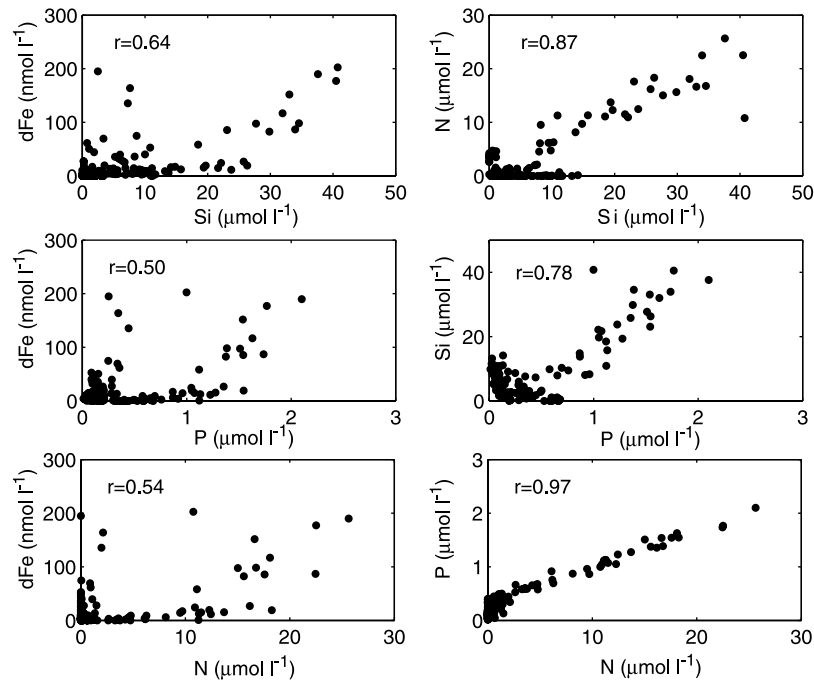


Figure 7. Scatterplots of nutrient-nutrient and iron-nutrient relationships from discrete (acidified) bottle samples collected from the underway surface water pumping system. The correlation coefficient (r) is shown on each plot ($n = 122$ samples).

greater nearshore at TR1, but greater offshore at TR3 (Figure 10 and Table 1). A small-scale anomaly was observed along TR3 in the temperature and salinity data between 45 and 50 km from shore, with an enrichment of Fe and N observed at the seaward edge of this feature (Figure 10).

3.5. Fast Repetition Rate Fluorometry

[32] The photosynthetic competency parameter, F_v/F_m , displayed strong diel variability, with high values at night and low values during the day. This behavior has been observed before [e.g., Behrenfeld and Kolber, 1999] and is most likely caused by nonphotochemical quenching at high light levels. At irradiances below $500 \text{ W m}^{-2} \text{ d}^{-1}$, F_v/F_m decreased roughly linearly with increasing light, but there was too much scatter in this relationship for it to be used to light correct the F_v/F_m data. We therefore restrict our analysis to FRRf measurements made between 21:00 and 05:00.

[33] The ratio F_v/F_m reaches a maximum value of 0.65 under optimal conditions, and deviations from this ratio have been interpreted as symptomatic of physiological stress, most notably nutrient limitation [Greene *et al.*, 1994]. In the present study, nighttime F_v/F_m varied between 0.4 and 0.6, with a mean of 0.48, suggesting a range from nutrient-replete to mildly nutrient-stressed phytoplankton. A similar range was observed on a transect between the Sargasso Sea and Delaware Bay [Geider *et al.*, 1993a], while values of 0.25 are typical of the Fe-limited equatorial Pacific [Behrenfeld *et al.*, 1996; Behrenfeld and Kolber, 1999]. Although there was a trend to lower values away from the coast, at least south of 45°N (Figure 10 and Figure 11d), overall, no correlation was found between F_v/F_m and ambient nutrient concentrations, or between F_v/F_m and temperature or salinity (not shown). The lowest values of nighttime F_v/F_m in this study (~ 0.4) were measured at stations CR7, CR8 and FM8 (Table 2).

Both dFe and Si concentrations were relatively low at these stations and the low F_v/F_m might reflect either mild Fe stress or mild Si stress (or some other stressor). Experiments with phytoplankton cultures suggest the ratios of maximal and minimum fluorescence to chlorophyll *a*, F_o/chl and F_m/chl , in dark adapted cells should increase under Fe and NO_3 limitation [Geider *et al.*, 1993b], decrease under Si limitation [Lippemeier *et al.*, 1999], and be unaffected by P limitation [Geider *et al.*, 1993b]. We have evaluated these parameters at all sites where nighttime F_v/F_m measurements were made at CTD stations, enabling a match between average continuous FRRf parameters (while on station) and chlorophyll *a* measured in the surface Rosette sample (Table 2). Although the data are limited, the ratios F_o/chl and F_m/chl at CR7 and FM8 were the highest of any of the stations, which suggests the low F_v/F_m observed at these stations is unlikely to be due to Si limitation [Lippemeier *et al.*, 1999]. At FM8, the low N and (relatively) low dFe, low F_v/F_m and high F_o/chl are consistent with both N and Fe nutrient stress [Geider *et al.*, 1993b].

4. Discussion

[34] Iron and nitrate concentrations off Oregon displayed complex spatial patterns in all dimensions. These distributions are clearly influenced by multiple factors, including topography, shelf geometry, and the magnitude and variability (spatial and temporal) of wind forcing. The following discussion focuses on mechanisms of iron inputs to the Oregon coastal region, and their biological implications.

4.1. Iron Sources

[35] The upwelling origin of surface water nitrate is well known from previous studies of coastal upwelling systems

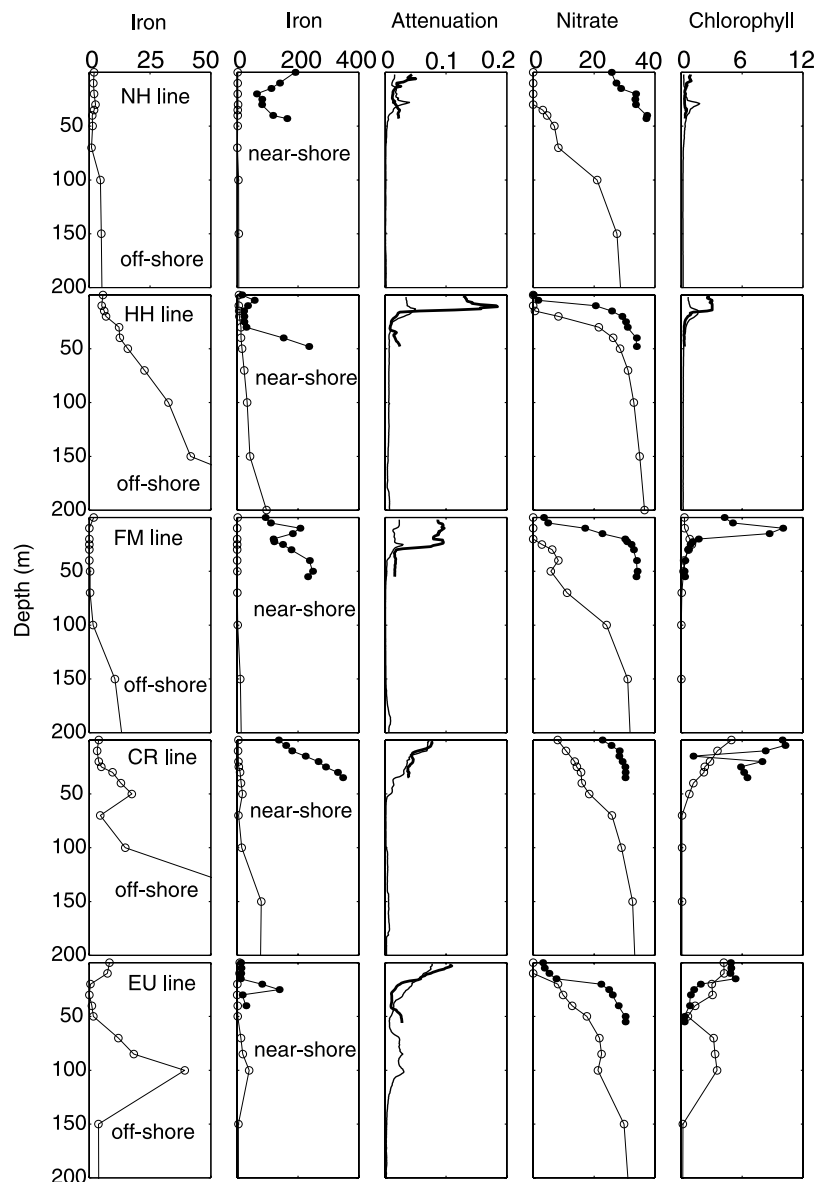


Figure 8. Vertical profiles of density anomaly (σ_0 ; kg m^{-3}), nitrate + nitrite (N) ($\mu\text{mol L}^{-1}$), chlorophyll *a* ($\mu\text{g L}^{-1}$), and dissolvable iron (dFe) (nmol L^{-1}) at the offshore (open symbols and thin lines) and nearshore (solid symbols, thick lines) ends of the lines sampled in July 1999. The offshore dFe profiles are replotted in the last panel to enlarge the scale. Station lines are presented top to bottom from north to south, with station locations shown in Figure 3c. On the NH and HH lines, chlorophyll *a* was estimated from in vivo fluorescence using the relationship between fluorescence and extracted chlorophyll *a* derived from all other casts. In general, less than 20 hours separated sampling the offshore and the nearshore stations, except along the NH line, where the offshore station was sampled 4 days before the nearshore station.

[e.g., Chavez *et al.*, 1991; Hayward and Venrick, 1998] and can be seen here, for example, in the similarity between density and nitrate profiles (e.g., Figure 8). Along all sampling lines, N levels at the nearshore station were less than or equal to the highest concentrations found in the top 200 m at the offshore station (Figure 8), which is consistent with an offshore, deep-water origin for nearshore N. In contrast to N, surface water underway Fe and nearshore dFe at all depths along most lines were higher than in offshore profiles, confirming the existence of iron sources distinct from the upwelling that delivers N to surface waters [Martin

and Gordon, 1988]. Here we evaluate three sources of Fe to Oregon surface waters: shelf sediments, Fe-enriched upwelling source waters, and the Columbia River, with an emphasis on how iron inputs relate to wind forcing and therefore nitrate supply (Table 3). We have no evidence to suggest a significant input of Fe from atmospheric sources, but note that they may be important locally, particularly near industrial centers [Hardy *et al.*, 1985].

4.1.1. Shelf Sediments

[36] Shelf sediments have been identified as the main source of Fe to the upwelling region off central California

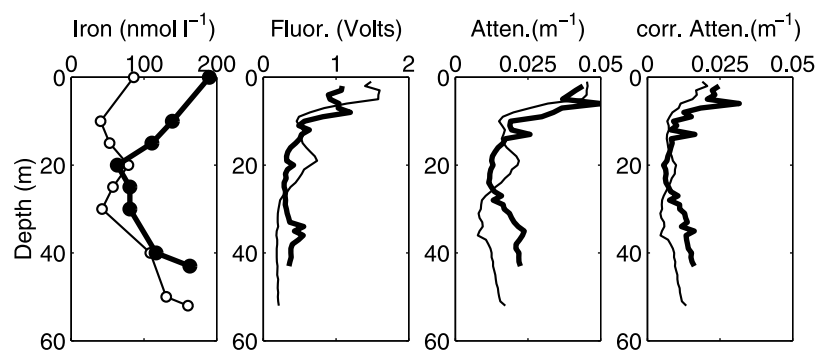


Figure 9. Vertical profiles of dissolvable iron (dFe) (nmol L^{-1}), fluorescence (Volts), beam attenuation (m^{-1}), and (d) beam attenuation corrected for chlorophyll, from stations at 9 km (thin line, open symbols) and 5 km (thick line, solid symbols) from shore along the NH line.

[Johnson *et al.*, 1999]. The importance of the shelf in supplying iron to California coastal waters is highlighted by the finding that north of Monterey Bay, where the continental shelf extends 20–50 km from shore, surface waters are iron-replete, whereas off the Big Sur coast, where the shelf extends only several km, surface waters are iron-depleted [Bruland *et al.*, 2001]. The high Fe concentrations found in this study over the broad shelf region of Heceta Bank are an indication of the importance of sedimentary Fe sources off Oregon. However, the mechanism by which sediment-derived Fe is introduced to surface waters is not well understood. Based on our observations, we propose three such mechanisms: (1) wind mixing, (2) outcropping of the bottom boundary layer, and (3) thickening of the bottom mixed layer.

[37] Input of sedimentary Fe to surface waters through bottom-reaching, wind-induced vertical mixing is likely to be important only in nonstratified water columns, very near-shore, and at high wind speeds. This mode of Fe input will be coupled to N input only when strong winds are upwelling favorable. Such conditions may have occurred nearshore at the CR line in July 1999, where a profile of dFe showed a linear increase with depth, suggesting a sedimentary source. Although winds at the time of sampling were not extremely

strong ($\sim 7 \text{ m s}^{-1}$ from the ship and the CARO3 lighthouse), the wind stress may have been sufficient to resuspend bottom sediments and their associated particulate and dissolved Fe because the water column was not stratified. The very low surface water Fe measured underway at this site, in contrast to the high dFe and N values, suggests either the mixing process supplied only particulate Fe from sediments, or consumption and scavenging of dissolved Fe was very rapid.

[38] Another way for sediment and surface water to interact is if the thickness of the bottom mixed layer (BML, a vertically homogeneous layer above the bottom) increases until it intersects the surface. Sediment-rich (and therefore, presumably, iron rich), nepheloid layers are often associated with BMLs. Observations from the northern California and Oregon shelves have shown that suppressed near-bottom vertical mixing, and hence thin BMLs, prevail during upwelling conditions, while enhanced vertical mixing and thick BMLs prevail during downwelling conditions [Pak and Zaneveld, 1977; Lentz and Trowbridge, 1991]. A BML develops rapidly following the onset of downwelling conditions [Pak and Zaneveld, 1977; Lentz and Trowbridge, 1991], which means even short-term wind reversals may lead to resuspension of Fe. The frequency of wind reversal events may therefore be a critical parameter in determining

Table 1. Discrete Nutrient Analyses From Along the High-Resolution Underway Transects Presented in Figure 10

Transect	Latitude, °N	Longitude, °W	Distance, km	P, $\mu\text{mol L}^{-1}$	Si, $\mu\text{mol L}^{-1}$	N, $\mu\text{mol L}^{-1}$	dFe, nmol L^{-1}
TR1							
	41.90	−124.65	49.7	0.4	1.2	0.1	<0.3
	41.90	−124.58	41.9	0.5	<0.2	2.6	<0.3
	41.90	−124.53	35.4	0.6	<0.2	3.3	<0.3
	41.90	−124.43	25.2	1.1	10.9	11.3	0.7
	41.90	−124.38	19.1	1.1	18.5	11.1	58.4
	41.90	−124.32	12.2	1.6	32.0	18.1	117.0
TR2							
	44.01	−124.19	6.1	0.3	2.5	<0.1	194.9
	44.05	−124.24	11.6	0.3	0.2	0.3	27.5
	44.09	−124.29	17.5	0.3	4.5	1.4	13.2
	44.13	−124.33	22.9	0.7	10.3	6.3	9.3
	44.19	−124.41	32.6	0.1	1.9	<0.1	44.0
TR3							
	44.87	−124.28	26.4	0.13	6.37	1.49	28.0
	44.73	−124.52	50.9	0.10	5.88	<0.1	31.9
	44.65	−124.65	72.2	0.10	8.35	<0.1	36.1

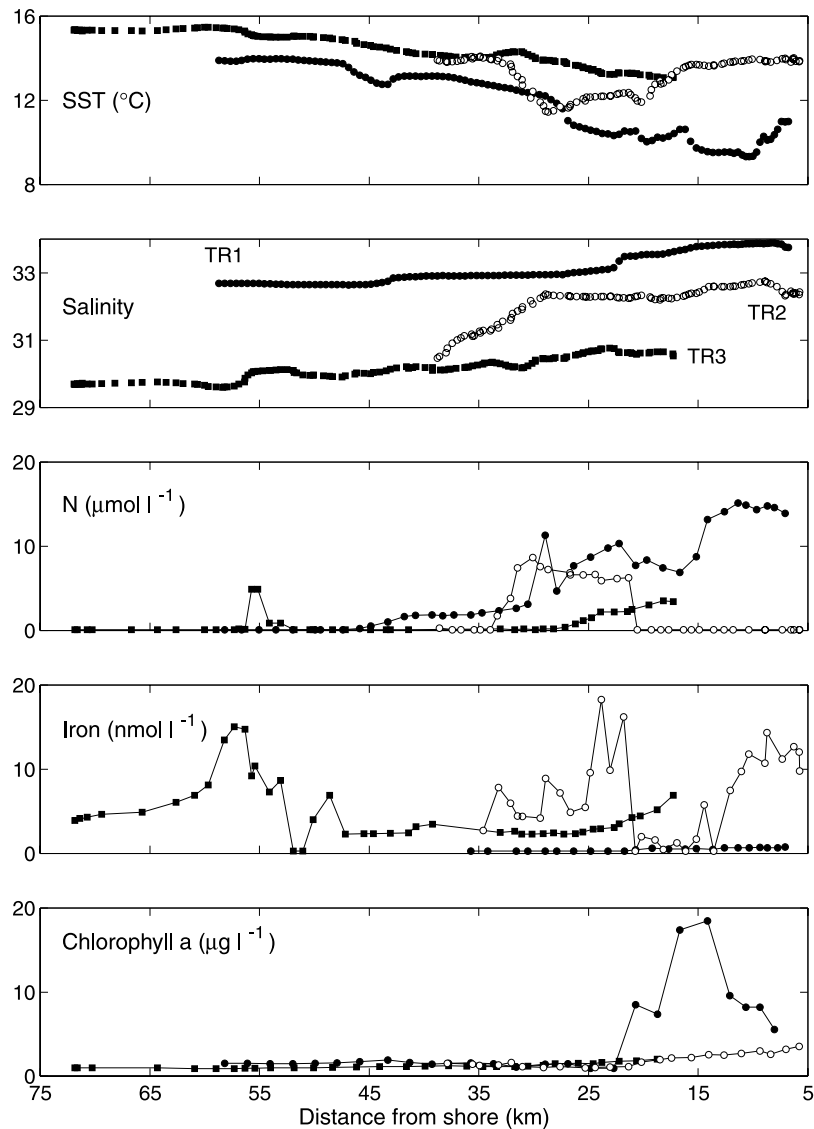


Figure 10. Transects TR1 (solid circles), TR2 (open circles), and TR3 (solid squares) showing surface water properties measured underway in July 1999: Chlorophyll *a* ($\mu\text{g L}^{-1}$) was derived from in vivo fluorescence. For locations, see dark bars in Figures 1 and 3. Analyses from discrete samples along these transects are presented in Table 1.

Fe inputs in coastal upwelling systems. This mechanism of iron input also helps explain the apparent decoupling between N and Fe distributions (e.g., Figure 6c), since it provides Fe input during downwelling, precisely when N inputs are minimal. Temporal variability in the height of the BML could also provide an explanation for the middepth minimum in dFe and particle concentration profiles observed at nearshore stations on the NH line at the onset of upwelling conditions (e.g., Figure 9). It is conceivable that during downwelling conditions, which preceded sampling at these NH stations, the BML thickened and the entire water column became turbid and iron-rich. With the onset of upwelling, the middepth minimum could then have been generated as an intermediate layer of clear, iron-poor water penetrated onto the shelf [Pak and Zaneveld, 1977; Lentz and Trowbridge, 1991].

[39] In the absence of vertical mixing, diffusion of Fe from sediments will reach at most several cm above the

sediment-water interface [Kremling and Petersen, 1978], and will not be easily entrained in the onshore flow. However, recent models [Allen et al., 1995] and observations [van Geen et al., 2000; Takesue and van Geen, 2002], suggest a substantial portion of upwelling flow occurs in the bottom boundary layer (BBL) and outcrops in very shallow waters near the coast. Therefore, even over steep topography (narrow shelf), some portion of an N-rich upwelling plume always interacts with the shelf where it may become enriched in Fe. Outcropping of the BBL may therefore explain the high dFe concentrations measured very nearshore on the FM line, in N-rich, recently upwelled waters. This mechanism could provide an alternative explanation for middepth minimum observed in the dFe profiles at shelf stations along the NH line at the onset of upwelling (e.g., Figure 9). Under this scenario, high-Fe waters outcropped within several km from shore during intense upwelling of

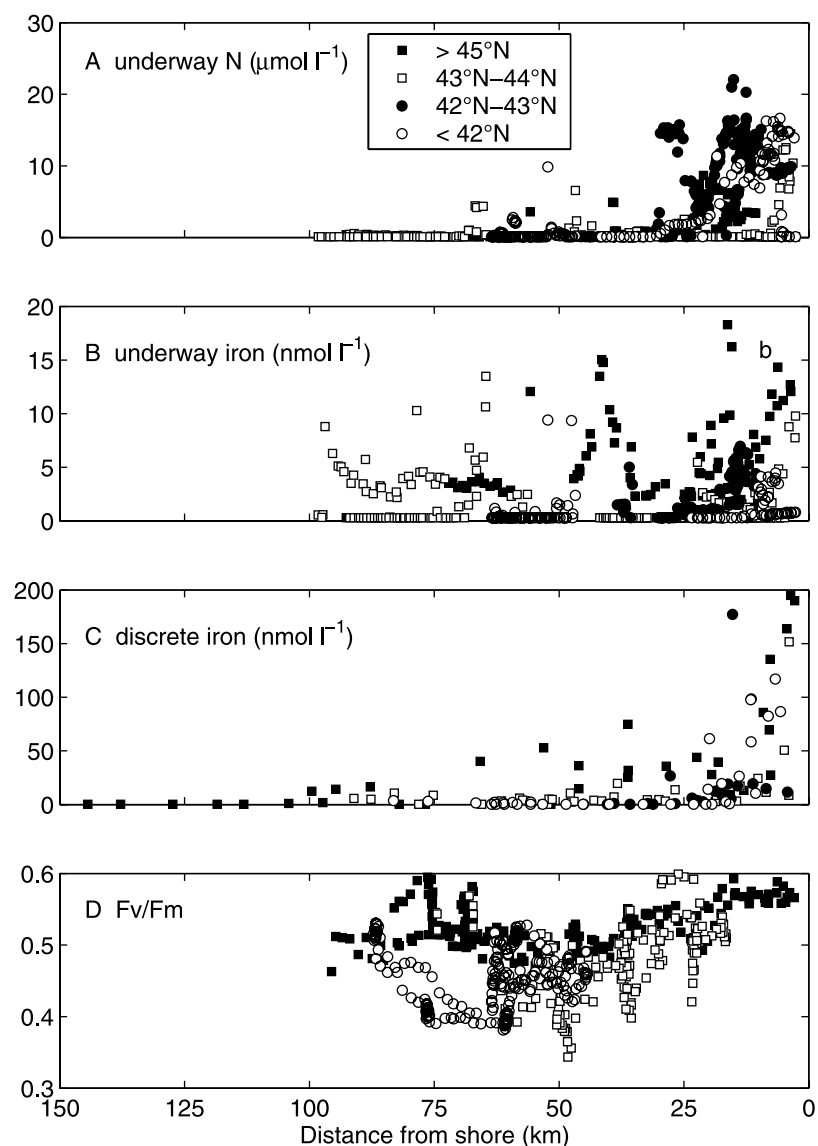


Figure 11. The cross-shelf distribution of (a) N (measured underway), (b) Fe (measured underway), (c) dFe (measured in discrete acidified samples), and (d) underway Fv/Fm measured at night (between 2100 and 0500) during the July 1999 survey. Data from four latitudinal bands are distinguished by different symbols.

the BBL, and were then transported offshore in the surface Ekman flow, over relatively less Fe-rich waters, to produce a middepth minimum in dFe.

4.1.2. Enrichment of Offshore Waters

[40] The work of *Martin and Gordon* [1988] off central California suggests that in the absence of shelf interaction, upwelling of deep offshore water cannot supply sufficient Fe to surface waters to support full consumption of the concurrently upwelled N, even if all forms of Fe are assumed to be bioavailable. Off Oregon, in contrast, we find dFe $>25 \text{ nmol L}^{-1}$ in 4 out of 5 profiles from stations seaward of the 1000 m isobath. This is about twice the amount of Fe required to support full consumption of the $\sim 25 \mu\text{mol L}^{-1}$ N present at the depth of upwelling in these source waters. The origin of these elevated levels of subsurface dFe off Oregon is not clear, and warrants further study. At the FM, EU and CR lines, the increases in dFe at depth are associated with slight increases in beam attenuation

(data not shown), which suggests the dFe may be largely particulate, and associated with resuspended sediment transported off the shelf [e.g., *Pak et al.*, 1980]. Another possibility is the transport of dissolved Fe from pore waters in fluidized flow along isopycnals as the result of sediment slumping [*Martin and Gordon*, 1988].

[41] Regardless of its origin, iron enrichment at middepth ($\sim 100 \text{ m}$) in offshore waters clearly represents an important iron source to nearshore surface waters in this region, via upwelling. This subsurface iron may also be mixed into surface waters on the outer shelf by a number of physical processes [e.g., *Klein and Coste*, 1984; *Dewey and Moum*, 1990; *Paduan and Niiler*, 1990; *Chavez et al.*, 1991], operating on perhaps very small spatial scales. The small anomaly observed in Fe and N along TR3 may have been the result of such a process, where N and Fe were brought to the surface by enhanced vertical mixing associated with the SST and salinity front, perhaps in response to wind forcing

Table 2. Nutrient and FRRf Data From CTD Stations Occupied at Night^a

Station	Latitude, °N	Longitude, °W	Chl <i>a</i>	Si	P	N	dFe	Fo/chl	Fm/chl	Fv/Fm
CR 7	41.90	-125.00	2.08	<0.2	0.5	3.0	1.5	276.6	462.5	0.40
CR 8	41.90	-125.20		<0.2	0.7	2.7	3.1			0.40
CR 9	41.90	-125.33	4.95	2.2	0.8	8.0	3.9	134.6	280.1	0.52
FM 5	43.22	-124.67	0.77	3.0	<0.1	<0.1	8.4	184.8	363.3	0.49
FM 6	43.22	-124.75								0.55
FM 7	43.22	-124.83	0.40	3.0	<0.1	<0.1	3.2	208.0	364.6	0.43
FM 8	43.22	-125.00	0.32	0.2	<0.1	<0.1	1.9	240.8	391.2	0.39
HH 3	44.00	-124.60		3.5	0.1	<0.1	19.6			0.51
HH 4	44.00	-124.80	0.71	2.9	<0.1	<0.1	10.7	132.3	248.6	0.47
HH 5	44.00	-125.00	0.90	3.0	<0.1	<0.1	4.1	106.8	233.2	0.54
HH 6	44.00	-125.10								0.55

^aSurface chlorophyll *a* ($\mu\text{g L}^{-1}$; extracted, not estimated from in vivo fluorescence), macronutrients ($\mu\text{mol L}^{-1}$), dissolvable iron (dFe and nmol L^{-1}), and photosynthetic parameters (measured by the underway FRRf). FRRf data acquired every 4 min were averaged over each station occupation. The dFe value at all stations except CR7 and CR9 is from discrete surface samples collected at station locations during underway transits.

across the front [Klein and Coste, 1984; Chavez *et al.*, 1991; Franks and Walstad, 1997].

4.1.3. Columbia River

[42] The presence of the Columbia River may account for the high iron levels off Oregon, compared to central California. The average discharge from the Columbia River at the Dalles, Oregon, in July 1999 was $7112 \text{ m}^3 \text{ s}^{-1}$ (<http://waterdata.usgs.gov>), which is over 10 times the discharge of the largest river in California (the Sacramento) at the same time ($630 \text{ m}^3 \text{ s}^{-1}$; California Department of Water Resources). The high dFe observed as far as the 1000 m isobath in low-salinity, high-silicate water along 45°N is a strong indication that iron from the Columbia River is transported hundreds of kilometers downstream. We have not made measurements of Fe in the Columbia River itself, but a USGS program reported dissolved Fe at $\sim 200 \text{ nmol L}^{-1}$ in July at 3 sites about 140 km upstream from the mouth [Fuhrer *et al.*, 1996], while earlier measurements of dissolved Fe in the Columbia River, compiled by Riedel *et al.* [1984], range from 9 to 2800 nmol L^{-1} . More data are needed, but it appears iron in the Columbia River estuary may exhibit the near-conservative behavior found in some estuaries with rapid flushing [Mayer, 1982b], rather than being lost through coagulation [Sholkovitz *et al.*, 1978].

[43] Iron input from the Columbia River plume is important because it represents a source of iron to waters seaward of the shelf break. Furthermore, the Fe at 45°N associated with the Columbia River plume is probably in a smaller size fraction than Fe associated with resuspended sediment, since larger particles would have settled out of the plume during its ~ 20 day [Huyer, 1983] transit from the river mouth. This is consistent with the high levels of Fe measured underway in the Columbia River plume, since our underway FIA system would probably not detect iron associated with large (>colloidal) particles. The presence of the Columbia River may

also contribute to the shelf sediment source of Fe by exporting Fe-rich particles accumulated in the estuary [Mayer, 1982b; Johnson *et al.*, 2001], or by contributing to rapid sediment accumulation and hence reducing conditions conducive to Fe flux from the sediments [Trefry and Presley, 1982]. The contrast between deep dFe concentrations offshore of California and Oregon may be due in part to the presence of the Columbia River, which produces an extensive band of fine sediment on the shelf [e.g., Gross *et al.*, 1967]. Composite SeaWiFS images for July 1998 and July 1999 (not shown), both show high phytoplankton biomass near the mouth of the Columbia River which suggests the river, which provides iron, silicic acid and a stable surface layer, may play an important role in maintaining biological productivity over the Oregon shelf.

4.2. Biological Implications

[44] This study was undertaken in part to evaluate whether iron might be a limiting nutrient off Oregon, as it can be in waters off central California [Hutchins and Bruland, 1998; Hutchins *et al.*, 1998]. Our data suggest it is not, except possibly on the outer shelf. Compared to open ocean environments and the HNLC waters observed off central California [Hutchins and Bruland, 1998; Hutchins *et al.*, 1998], iron concentrations, both underway and dissolvable, were high off Oregon. At these nanomolar concentrations Fe is unlikely to be rate limiting, even for coastal phytoplankton [Sunda and Huntsman, 1995]. Another manifestation of iron limitation is Liebig limitation, in which the size of a phytoplankton bloom is limited by the concentration of the least available nutrient, relative to demand. The amount of Fe needed to support full consumption of upwelled nitrate varies strongly as a function of the ambient iron concentration [Bruland *et al.*, 2001], and this makes it difficult to predict the Fe:N (or Fe:P) input ratio at which

Table 3. Proposed Sources and Mechanisms of Iron Inputs to Surface Waters and Their Relationship to Nitrate Input

Iron Source	Mechanism	Winds	Nitrate Input
Shelf sediments	wind-induced mixing	strong; equatorward or poleward	No
	thickening of bottom mixed layer/bottom nepheloid layer	weak or poleward	No
	outcropping of the bottom boundary layer	strong; equatorward	Yes
Offshore deepwater	isopycnal shoaling; diapycnal vertical mixing	strong; equatorward	Yes
Columbia River	plume transport	any	small

Liebig limitation by iron applies. A further complication is that a one-time measurement of Fe and N at a given location says nothing about the initial ratio at which these nutrients were added to the system.

[45] The best way to assess the nutrient limitation status of the phytoplankton community may be with nutrient addition/incubation experiments. However, fast repetition rate fluorometry (FRRf) can be used to assess (and map) the physiological status of the phytoplankton community. Overall, the relatively high (0.4–0.6) nighttime values of Fv/Fm found during this study are not consistent with severe (rate) nutrient limitation of any kind. It also appears unlikely that iron input was Liebig-limiting the development of phytoplankton blooms off Oregon in July 1999. We note that the largest bloom observed in this study, south of Cape Blanco, was not coincident with the region of greatest iron inputs (over and north of Heceta Bank), but rather with the region of strongest upwelling (lowest SST, strongest shoaling of the pycnocline).

[46] Another approach to assess nutrient limitation is to consider the time course of an upwelled parcel of water [Bruland *et al.*, 2001]. For example, along TR1, on the CR line, underway iron fell to below our detection limit closer to shore than did nitrate, at roughly the same distance from shore that the chlorophyll concentration fell to low levels. One interpretation of these observations is that as the nearshore phytoplankton bloom aged and was advected offshore in the surface Ekman layer, it came to an end about 25 km from shore due to lack of iron. Indeed, the FRRf data (low Fv/Fm and high Fo/chl) from offshore waters along the CR line were consistent with mild iron stress. The low concentrations of Si observed in this region, relative to N, may even be the result of an increased Si:N uptake ratio in Fe-stressed diatoms [Hutchins and Bruland, 1998; Takeda, 1998]. Thus, despite the relatively high iron concentrations in offshore waters of the Oregon upwelling region, our analysis of Fv/Fm and Fo/chl at CTD stations, and the cross-shelf distribution of Fe, N and chlorophyll does suggest iron can exert some physiological control on the phytoplankton community. In the hierarchy of Hutchins *et al.* [1998] these may be type 2, or “slightly Fe-stressed”, communities.

[47] From the difference between Fe concentrations measured underway and in acidified samples, and from the coherence between profiles of particle concentration and dFe, we conclude that much of the iron in the nearshore environment is associated with suspended particles. This means iron concentrations in the euphotic zone will depend critically on relative rates of solubilization of Fe from particles [e.g., Wells and Mayer, 1991; Johnson *et al.*, 1994; Barbeau *et al.*, 1996; Maranger *et al.*, 1998] and sinking rates of particulate Fe in the offshore flowing surface layer. The observation that the same intensity of fluorescence-corrected beam attenuation was associated with a higher concentration of dFe nearshore than offshore (e.g., Figure 9) may indicate ‘stripping’ of Fe from particulate phases as they move across the shelf [Johnson *et al.*, 1997]. Barber and Smith [Barber and Smith, 1981] have proposed that the two-layered flow of upwelling systems makes them important sites for recycled production. The same may be true for Fe, in the sense that any particulate Fe which sinks into the BBL can be entrained in the onshore

flow and upwelled again to the surface where it may be subjected to further solubilization.

[48] The strong baroclinic jets of the Coastal Transition Zone (CTZ) off California do not transport a significant amount of coastally upwelled nitrate to the ocean interior [Chavez *et al.*, 1991], and this also appears to be the case off Oregon. In July 1999, N enrichment did not extend further than ~50 km from the coast (Figure 10 and Figure 11a), even south of Cape Blanco, where the coastal jet moves offshore [Barth *et al.*, 2000]. Throughout the survey area, high dFe levels were generally restricted close to shore, but elevated levels of Fe were measured underway at all distances from shore (Figure 10 and Figures 11b and 11c), especially north of Cape Blanco, perhaps reflecting the diversity (and abundance) of iron sources. The potential for Fe export from the coastal ocean probably depends on the form of nearshore Fe. Iron that has been solubilized from lithogenic particles [Johnson *et al.*, 1997] and incorporated into the dissolved or biogenic pool may be more likely to escape sedimentation over the shelf, and be exported to the ocean interior.

5. Conclusions

[49] The high-resolution surface water transects and vertical profiles of chemical and biological parameters presented here provide insight into the magnitude, mechanisms and consequences of iron and nitrate inputs to surface waters of the Oregon upwelling system. Our results support conclusions for central California that shelf sediments are an important source of Fe to coastal upwelling systems [Johnson *et al.*, 1999]. Sedimentary iron, largely in the particulate form, is added to surface waters through wind-induced vertical mixing, thickening of the bottom mixed layer, and upwelling through the bottom boundary layer. Off Oregon, iron input associated with the Columbia River is also important. A full description of Fe inputs to the Oregon upwelling system will require a better understanding of the magnitude, reactivity and variability of Fe inputs from the Columbia River. Middepth waters off the Oregon shelf appear to contain significantly more total Fe than waters off central California, and this offshore enrichment also contributes Fe to surface waters. As a result of large riverine inputs, a relatively wide shelf and offshore enrichment of deep waters, iron concentrations off Oregon, both labile and total, are generally high, and not likely to be limiting biological production. However, relatively high-nitrate ($>10 \mu\text{mol L}^{-1} \text{NO}_3$), low-iron ($<0.5 \text{nmol L}^{-1}$) waters do exist off Oregon, as they do off California [Hutchins and Bruland, 1998; Hutchins *et al.*, 1998], and this may influence phytoplankton physiology and productivity seaward of the shelf break. The source and mechanism of iron input is expected to influence the form of iron in surface waters, its decoupling from macronutrients, and its residence time. Future work should examine seasonal changes in iron inputs and possible iron limitation along the Oregon coast [as was done recently for Monterey Bay Johnson *et al.*, 2001] as well as characterize the biological availability of iron associated with the various input mechanisms described in this paper.

[50] **Acknowledgments.** We thank the officers and crew of the R/V *Wecoma*, who went to great lengths to assist with the underway operations.

N. Ventriello and C. Ho acquired and reduced the FRRF data. AVHRR data were provided by P.T. Strub (O.S.U.) under funding by the U.S. GLOBEC program. J. Fleischbein kindly provided the CTD data. Discussions with J. Barth, K. Bruland, B. Hales, R. Letelier, and P. Strutton were very helpful. This work was funded by the Office of Naval Research (NOO014-99-1-0279 to AvG and JM) and by a fellowship (awarded to ZC) from the Fonds pour la Formation de Chercheurs et l'Aide à la Recherche (Québec). This is LDEO publication number 6315.

References

- Allen, J. S., P. A. Newberger, and J. Federiuk, Upwelling circulation on the Oregon continental shelf, I, Response to idealized forcing, *J. Phys. Oceanogr.*, **25**, 1843–1866, 1995.
- Anderson, L., Simultaneous spectrophotometric determination of nitrite and nitrate by flow injection analysis, *Anal. Chim. Acta*, **110**, 123–128, 1979.
- Arthur, R. S., On the calculation of vertical motion in eastern boundary currents from determinations of horizontal motion, *J. Geophys. Res.*, **70**, 2799–2803, 1965.
- Barbeau, K., J. W. Moffett, D. A. Caron, P. L. Croot, and D. L. Erdner, Role of protozoan grazing in relieving iron limitation of phytoplankton, *Nature*, **380**, 61–64, 1996.
- Barber, R. T., and R. L. Smith, Coastal upwelling ecosystems, in *Analysis of Marine Ecosystems*, edited by A. R. Longhurst, pp. 31–68, Academic, San Diego, Calif., 1981.
- Barth, J. A., S. D. Pierce, and R. L. Smith, A separating coastal upwelling jet at Cape Blanco, Oregon and its connection to the California Current System, *Deep Sea Res., Part II*, **47**, 783–810, 2000.
- Behrenfeld, M. J., and Z. S. Kolber, Widespread iron limitation of phytoplankton in the South Pacific Ocean, *Science*, **283**, 840–843, 1999.
- Behrenfeld, M. J., A. J. Bale, Z. S. Kolber, J. Aiken, and P. G. Falkowski, Confirmation of iron limitation of phytoplankton photosynthesis in the equatorial Pacific Ocean, *Nature*, **383**, 508–511, 1996.
- Boyle, E. A., J. M. Edmond, and E. R. Sholkovitz, The mechanism of iron removal in estuaries, *Geochim. Cosmochim. Acta*, **41**, 1313–1324, 1977.
- Boyle, E. A., S. S. Husteded, and B. Grant, The chemical mass balance of the Amazon plume, II, Copper, nickel and cadmium, *Deep Sea Res., Part I*, **29**, 1355–1364, 1982.
- Brink, K. H., J. H. Lacasse, and J. D. Irish, The effect of short-scale wind variations on shelf currents, *J. Geophys. Res.*, **99**, 3305–3315, 1994.
- Bruland, K. W., and E. L. Rue, Iron: Analytical methods for the determination of concentrations and speciation, in *The Biogeochemistry of Iron in Seawater*, edited by K. A. Hunt and D. R. Turner, pp. 255–289, chap. 6, John Wiley, New York, 2001.
- Bruland, K. W., E. L. Rue, and G. J. Smith, Iron and macronutrients in California coastal upwelling regimes: Implications for diatom blooms, *Limnol. Oceanogr.*, **46**, 1661–1674, 2001.
- Brzezinski, M. A., D. R. Philips, F. P. Chavez, G. E. Friederich, and R. C. Dugdale, Silica production in the Monterey, California upwelling system, *Limnol. Oceanogr.*, **42**, 1694–1705, 1997.
- Chavez, F. P., R. T. Barber, P. M. Kosro, A. Huyer, S. R. Ramp, T. P. Stanton, and B. R. Demendiola, Horizontal transport and the distribution of nutrients in the Coastal Transition Zone off northern California: Effects on primary production, phytoplankton biomass and species composition, *J. Geophys. Res.*, **96**, 14,833–14,848, 1991.
- Coale, K. H., et al., A massive phytoplankton bloom induced by an ecosystem-scale iron fertilization experiment in the equatorial Pacific Ocean, *Nature*, **383**, 495–501, 1996.
- Dewey, R. K., and J. N. Moum, Enhancement of fronts by vertical mixing, *J. Geophys. Res.*, **95**, 9433–9445, 1990.
- Franks, P. J. S., and L. J. Walstad, Phytoplankton patches at fronts: A model of formation and response to wind events, *J. Mar. Res.*, **55**, 1–29, 1997.
- Fuhrer, G., G. Tanner, J. Morace, S. McKenzie, and K. Skach, Water analysis of the lower Columbia River basin: Analysis of current and historical water-quality data through 1994, *USGS Water-Resour. Invest. 95-4294*, U. S. Geol. Surv., Portland, Oreg., 1996.
- Geider, R. J., R. M. Greene, Z. Kolber, H. L. Macintyre, and P. G. Falkowski, Fluorescence assessment of the maximum quantum efficiency of photosynthesis in the western North Atlantic, *Deep Sea Res., Part I*, **40**, 1205–1224, 1993a.
- Geider, R. J., J. Laroche, R. M. Greene, and M. Olaizola, Response of the photosynthetic apparatus of *Phaeodactylum tricornutum* (Bacillariophyceae) to nitrate, phosphate, or iron starvation, *J. Phycol.*, **29**, 755–766, 1993b.
- Gordon, L. I., J. C. Jennings, A. R. Ross, and J. M. Krest, A suggested protocol for continuous flow automated analysis of seawater nutrients (phosphate, nitrate, nitrite, and silicic acid) in the WOCE hydrographic program and the Joint Global Ocean Fluxes Study, *Rep. 93-1*, Oregon State Univ., Corvallis, 1995.
- Greene, R. M., Z. S. Kolber, D. G. Swift, N. W. Tindale, and P. G. Falkowski, Physiological limitation of phytoplankton photosynthesis in the eastern equatorial Pacific determined from variability in the quantum yield of fluorescence, *Limnol. Oceanogr.*, **39**, 1061–1074, 1994.
- Gross, M. G., D. A. McManus, and H.-Y. Ling, Continental shelf sediment, northwestern United States, *J. Sediment Petrol.*, **37**, 790–795, 1967.
- Hardy, J. T., C. W. Apts, E. A. Crecelius, and N. S. Bloom, Sea-surface microlayer metal enrichments in an urban and rural bay, *Estuarine Coastal Shelf Sci.*, **20**, 299–312, 1985.
- Hayward, T. L., and E. L. Venrick, Near-surface pattern in the California Current: Coupling between physical and biological structure, *Deep Sea Res., Part II*, **45**, 1617–1638, 1998.
- Hutchins, D. A., and K. W. Bruland, Iron-limited diatom growth and Si: N uptake ratios in a coastal upwelling regime, *Nature*, **393**, 561–564, 1998.
- Hutchins, D. A., G. R. DiTullio, Y. Zhang, and K. W. Bruland, An iron limitation mosaic in the California upwelling regime, *Limnol. Oceanogr.*, **43**, 1037–1054, 1998.
- Huyer, A., Coastal upwelling in the California Current system, *Prog. Oceanogr.*, **12**, 259–284, 1983.
- Johnson, K. S., K. H. Coale, V. A. Elrod, and N. W. Tindale, Iron photochemistry in seawater from the equatorial Pacific, *Mar. Chem.*, **46**, 319–334, 1994.
- Johnson, K. S., R. M. Gordon, and K. H. Coale, What controls dissolved iron concentrations in the world ocean?, *Mar. Chem.*, **57**, 137–161, 1997.
- Johnson, K. S., F. P. Chavez, and G. E. Friederich, Continental-shelf sediment as a primary source of iron for coastal phytoplankton, *Nature*, **398**, 697–700, 1999.
- Johnson, K., F. P. Chavez, V. A. Elrod, S. E. Fitzwater, J. T. Pennington, K. R. Buck, and P. M. Walz, The annual cycle of iron and the biological response in central California coastal waters, *Geophys. Res. Lett.*, **28**, 1247–1251, 2001.
- Klein, P., and B. Coste, Effects of wind-stress variability on nutrient transport into the mixed layer, *Deep Sea Res., Part A*, **31**, 21–37, 1984.
- Kosro, P. M., A poleward jet and an equatorial undercurrent observed off Oregon and northern California, during the 1997–98 El Niño, *Prog. Oceanogr.*, in press, 2002.
- Kremling, K., and H. Petersen, Distribution of Mn, Fe, Zn, Cd and Cu in Baltic seawater—A study on the basis of one anchor station, *Mar. Chem.*, **6**, 155–170, 1978.
- Lentz, S. J., and J. H. Trowbridge, The bottom boundary-layer over the northern California shelf, *J. Phys. Oceanogr.*, **21**, 1186–1201, 1991.
- Lippemeier, S., P. Hartig, and F. Colijn, Direct impact of silicate on the photosynthetic performance of the diatom *Thalassiosira weissflogii* assessed by on- and off-line PAM fluorescence measurements, *J. Plankton Res.*, **21**, 269–283, 1999.
- Maranger, R., D. F. Bird, and N. M. Price, Iron acquisition by photosynthetic marine phytoplankton from ingested bacteria, *Nature*, **396**, 248–251, 1998.
- Martin, J. H., and R. M. Gordon, Northeast Pacific iron distributions in relation to phytoplankton productivity, *Deep Sea Res., Part A*, **35**, 177–196, 1988.
- Mayer, L. M., Aggregation of colloidal iron during estuarine mixing: Kinetics, mechanism and seasonality, *Geochim. Cosmochim. Acta*, **46**, 2527–2535, 1982a.
- Mayer, L. M., Retention of riverine iron in estuaries, *Geochim. Cosmochim. Acta*, **46**, 1003–1009, 1982b.
- Measures, C. I., J. Yuan, and J. A. Resing, Determination of iron in seawater by flow injection analysis using in-line preconcentration and spectrophotometric detection, *Mar. Chem.*, **50**, 3–12, 1995.
- Morel, F. M. M., J. G. and Hering, *Principles of Aquatic Chemistry*, John Wiley, New York, 1993.
- Obata, H., H. Karatani, M. Matsui, and E. Nakayama, Fundamental studies for chemical speciation of iron in seawater with an improved analytical method, *Mar. Chem.*, **56**, 97–106, 1997.
- Paduan, J. D., and P. P. Niiler, A Lagrangian description of motion in northern California coastal transition filaments, *J. Geophys. Res.*, **95**, 18,095–18,109, 1990.
- Pak, H., and J. R. V. Zaneveld, Bottom nepheloid layers and bottom mixed layers observed on the continental-shelf off Oregon, *J. Geophys. Res.*, **82**, 3921–3931, 1977.
- Pak, H., J. R. V. Zaneveld, and J. Kitchen, Intermediate nepheloid layers observed off Oregon and Washington, *J. Geophys. Res.*, **85**, 6697–6708, 1980.
- Park, K., C. Osterberg, and W. Forster, Chemical budget of the Columbia River, in *The Columbia River Estuary and Adjacent Ocean Waters*, edited by A. Pruter and D. Alverson, pp. 123–135, Univ. of Wash. Press, Seattle, 1992.
- Parsons, T. R., M. Takahashi, and B. Hargrave, *Biological Oceanographic Processes*, 332 pp., Pergamon, New York, 1977.

- Riedel, G. F., S. L. Wilson, and R. L. Holton, Trace metals in the Columbia River estuary following the 18 May 1980 eruption of Mount St. Helens, *Pac. Sci.*, *38*, 340–348, 1984.
- Sholkovitz, E. R., E. A. Boyle, and N. B. Price, The removal of dissolved humic acids and iron during estuarine mixing, *Earth Planet. Sci. Lett.*, *40*, 130–136, 1978.
- Small, L., and H. Curl, The relative contribution of particulate chlorophyll and river tripton to the extinction of light off the coast of Oregon, *Limnol. Oceanogr.*, *13*, 84–91, 1968.
- Sunda, W. G., and S. A. Huntsman, Iron uptake and growth limitation in oceanic and coastal phytoplankton, *Mar. Chem.*, *50*, 189–206, 1995.
- Takeda, S., Influence of iron availability on nutrient consumption ratio of diatoms in oceanic waters, *Nature*, *393*, 774–777, 1998.
- Takesue, R. K., and A. van Geen, Nearshore circulation during upwelling inferred from the distribution of dissolved cadmium off the Oregon coast, *Limnol. Oceanogr.*, *47*, 176–185, 2002.
- Trefry, J. H., and B. J. Presley, Manganese fluxes from Mississippi delta sediments, *Geochim. Cosmochim. Acta*, *46*, 1715–1726, 1982.
- van Geen, A., R. K. Takesue, J. Goddard, T. Takahashi, J. A. Barth, and R. L. Smith, Carbon and nutrient dynamics during coastal upwelling off Cape Blanco, Oregon, *Deep Sea Res., Part II*, *47*, 975–1002, 2000.
- Vink, S., E. A. Boyle, C. I. Measures, and J. Yuan, Automated high resolution determination of the trace elements iron and aluminum in the surface ocean using a towed fish coupled to flow injection analysis, *Deep Sea Res., Part I*, *47*, 1141–1156, 2000.
- Waterbury, R. D., W. S. Yao, and R. H. Byrne, Long pathlength absorbance spectroscopy: Trace analysis of Fe(II) using a 4.5m liquid core waveguide, *Anal. Chim. Acta*, *357*, 99–102, 1997.
- Wells, M. L., and L. M. Mayer, Variations in the chemical lability of iron in estuarine, coastal and shelf waters and its implications for phytoplankton, *Mar. Chem.*, *32*, 195–210, 1991.
-
- Z. Chase, Monterey Bay Aquarium Research Institute, 7700 Sandholdt Road, Moss Landing, CA 95039, USA. (zanna@mbari.org)
- P. M. Kosro and P. A. Wheeler, College of Oceanic and Atmospheric Sciences, Oregon State University, Corvallis, OR 97331–5503, USA.
- J. Marra and A. van Geen, Lamont-Doherty Earth Observatory of Columbia University, P. O. Box 1000, Palisades, NY 10964, USA.

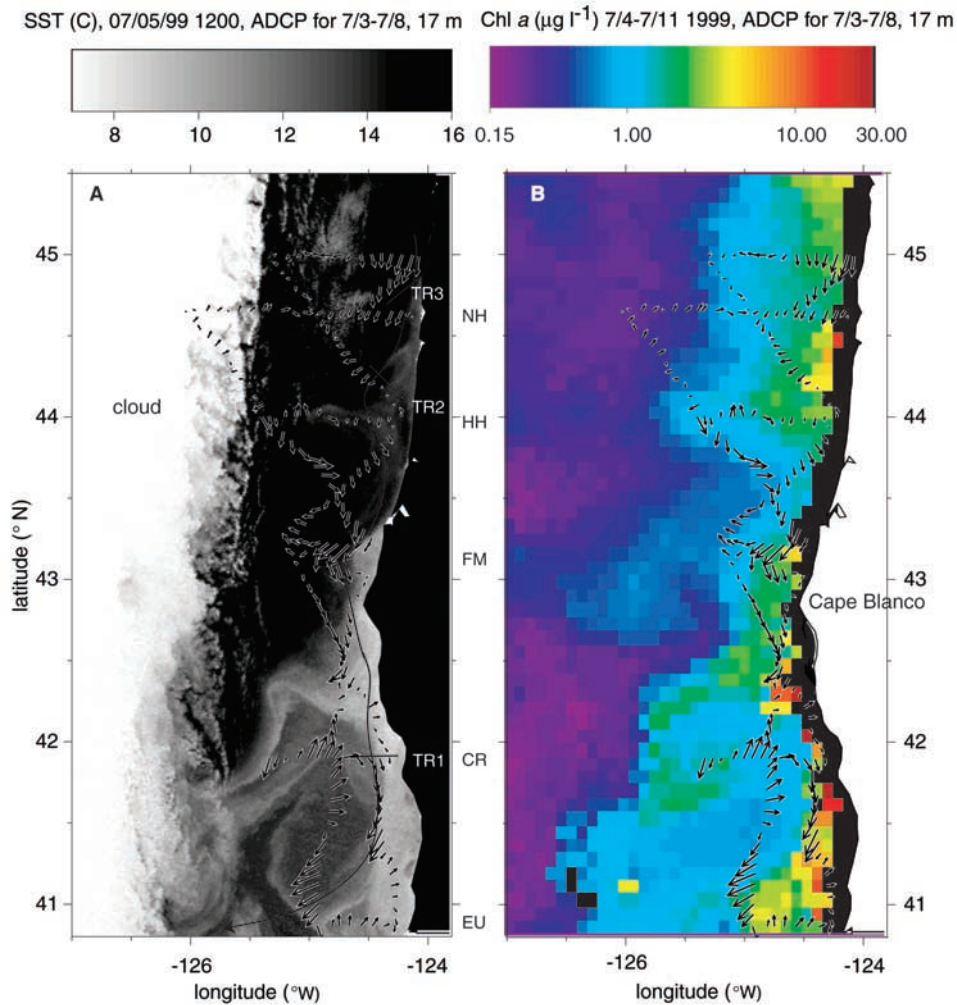


Figure 1. ADCP velocity vectors (longest arrow represents 42 cm/s) at 17 m between 3 and 8 July 1999 overlaid on satellite-derived (a) sea surface temperature ($^{\circ}\text{C}$) from 5 July and (b) an 8 day (7/4–7/11) composite of satellite-derived chlorophyll *a* concentration ($\mu\text{g L}^{-1}$). Chlorophyll is displayed on a logarithmic scale. There are no chlorophyll data in the black regions near the coast. A probable path of the coastal current has been subjectively drawn through the velocity vectors in Figure 1a. The locations of three transects where high-resolution data are examined more closely are also indicated in Figure 1a. Initials along the coast indicate the standard sampling lines of the Oregon GLOBEC program.

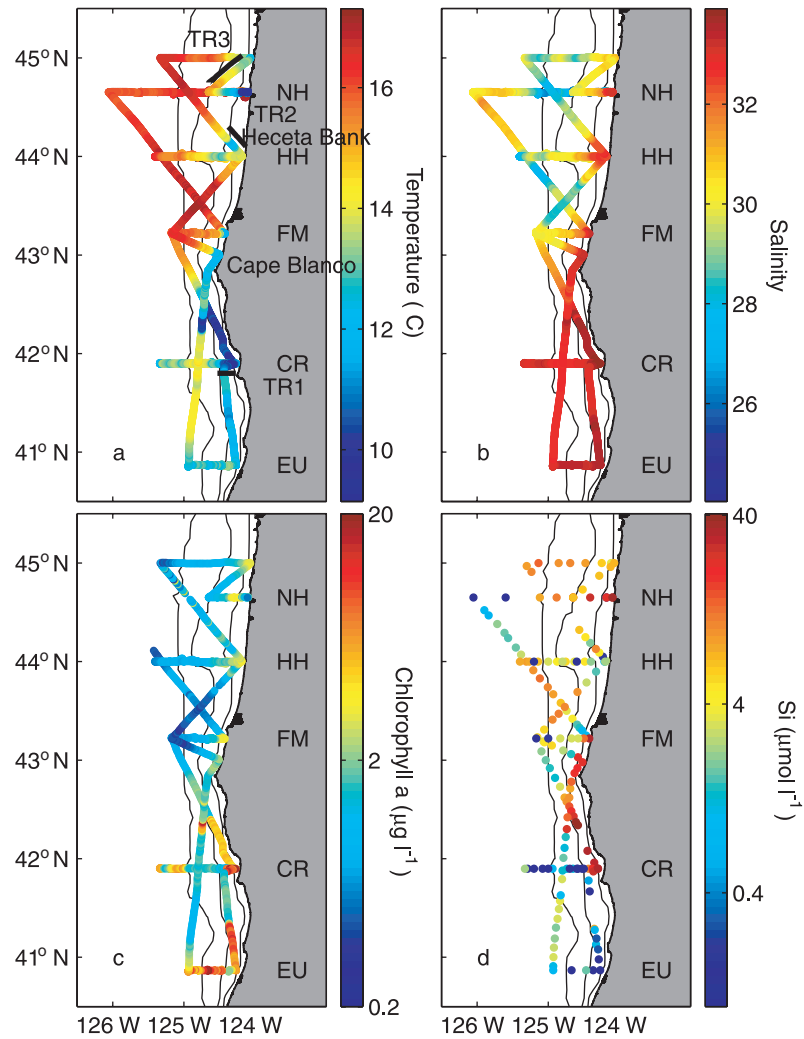


Figure 3. Surface water properties measured off Oregon during July 3–8, 1999. (a) Temperature ($^{\circ}\text{C}$), (b) salinity (psu), and (c) chlorophyll *a* ($\mu\text{g L}^{-1}$, estimated from *in vivo* fluorescence) were measured continuously while the ship was underway. (d) Silicate (silicic acid) was measured in discrete, acid-preserved samples in the laboratory. Where transects were covered twice during the cruise, the later data are plotted over the earlier data. Note the logarithmic color scale used for chlorophyll *a* and silicate concentrations. Contour lines represent the 50, 200, and 1000 m isobaths.

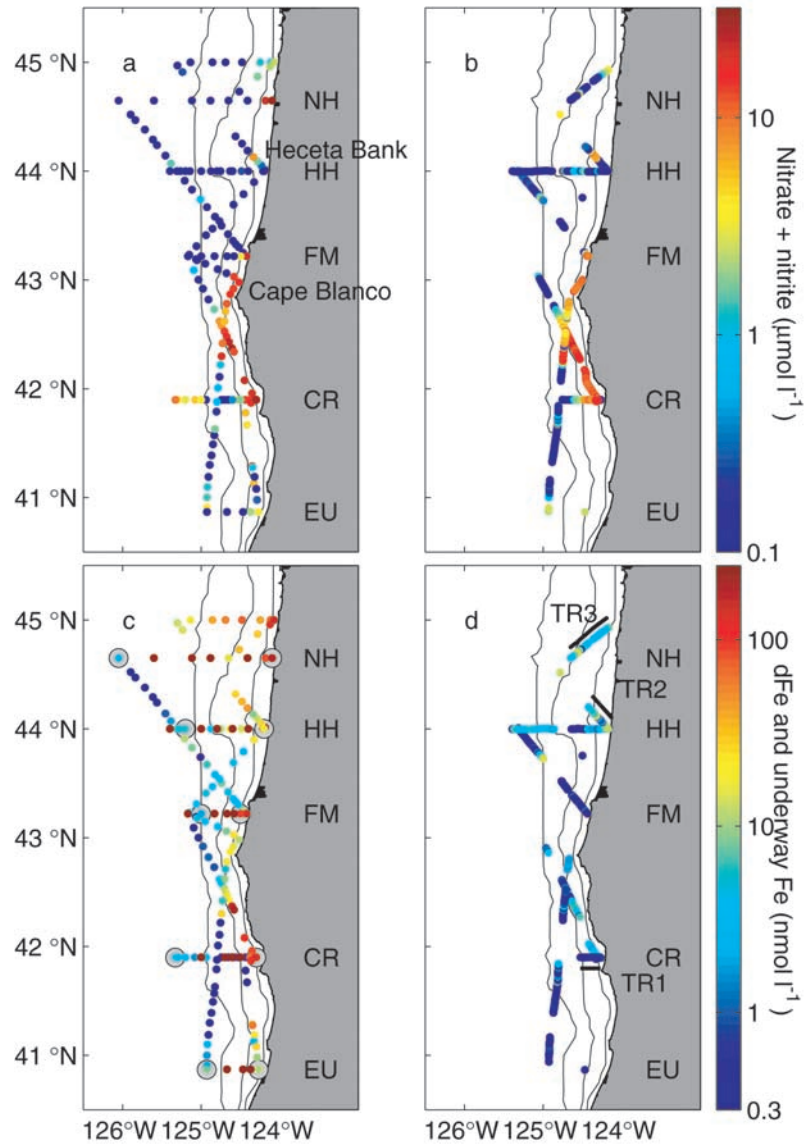


Figure 4. Surface water concentrations of (a) and (b) nitrate + nitrite (N) ($\mu\text{mol L}^{-1}$) and (c) and (d) iron (nmol L^{-1}) off Oregon, July 3–8, 1999, measured in discrete, acidified (pH 2) samples collected from the underway pumping system or (unacidified) surface rosette samples (Figures 4a and 4c) and at sea by flow injection analysis, without filtration or acidification (Figures 4b and 4d). Note the logarithmic color scale. Gray circles in Figure 4c indicate the location of CTD stations where vertical profiles of N and Fe were obtained.